

DOI: [10.5281/zenodo.15252570](https://doi.org/10.5281/zenodo.15252570)



Bathymetry Extraction from SPOT 7 Satellite Imagery with Semiparametric Regression

Kuncoro T. Setiawan¹, Devica Natalia BR Ginting², Maryani Hartuti¹, Masita D.M. Manessa³, Andy Indradjad⁴,
Ahmad Sutanto¹, Pingkan Mayestika Afgatiani^{1,5} Gathot Winarso¹ dan Nanin Anggraini²

¹Research Center for Geoinformatics, BRIN, Cibinong, Indonesia, 16911

²Research Center for Oceanography, BRIN, Jakarta 14430, Indonesia

³Department of Geography, Universitas Indonesia, Depok 16424, Indonesia

⁴Research Center for Satellite Technology, BRIN, Bogor, Indonesia, 16310

⁵Graduate School of Engineering and Science, University of the Ryukyus, Nishihara, Okinawa, Japan, 903-0213

* Correspondence: kunc002@brin.go.id

Published: 21 April 2025

Accepted: 16 April 2025

Received: 20 March 2025

Abstract: Bathymetry maps are essential for navigation and resource management, and as an intermediate product for mapping coastal marine habitats. Satellite-derived bathymetry (SDB) uses remote sensing technology to process reflection values from the bottom of the water to produce bathymetric information. This study aims to analyze the effect of bottom types of in-situ depth data on bathymetry estimation using semiparametric regression using spatial coordinates (Kanno-STR). We utilized two modified Kanno-STR methods, e.g., unconsidered and considered benthic habitats (coral reefs, seagrass, macroalgae, and substrates) on SPOT 7 data. The study area focused on the shallow water around Gili Trawangan, Gili Meno, and Gili Air Island, West Nusa Tenggara Province. For the first modification, the result shows that the coefficient of determination of the Kanno-STR method was 0.95, with an accuracy value of 78 % and a kappa coefficient value of 0.71. On the other hand, the second modification coefficient of determination on the Kanno-STR method was 0.84, with an accuracy value of 61% and a kappa coefficient value of 0.49. The interesting finding that SPOT 7 could penetrate up to 29.93 m. Separating benthic habitat cover into coral, seagrass, macroalgae, and substrate does not improve the accuracy of bathymetry results.

Keywords: : *Bathymetry, Semiparametric, Kanno-STR, SPOT 7.*

1. Introduction

Indonesia needs comprehensive bathymetry information to support its diverse marine activities as maritime country, including navigation, port development, and environmental conservation. Bathymetry information is crucial in economic development efforts as it aids in delineating national boundaries and asserting sovereignty over maritime territories (Lambach, 2022). Indonesia's enormous and diverse marine environment presents obstacles to obtaining comprehensive bathymetric data, particularly in shallow waters and areas with coral reefs (Dewi & Oktaviani, 2021). Traditional acoustic methods, such as single and multi-beam echo-sounding, are commonly used but costly and time-consuming with limitations in shallow areas (Dewi & Oktaviani, 2021; Jawak et al., 2015; Kanno et al., 2011). Hence, remote sensing imagery is considered to be a time-saving, low-cost, and wide-ranging solution for obtaining bathymetric information (Abdul Gafoor et al., 2022; Mohamed et al., 2017; Poliyapram et al., 2017; Wicaksono et al., 2024).

Remote sensing technology, especially optical imagery works on the spectrum of electromagnetic waves by utilizing sunlight. It has the potential to penetrate water depths up to 30 meters, particularly in clear water conditions (Jagalingam et al., 2015). The penetration of sunlight into a water body is significantly influenced by the water's ability to absorb sunlight, which is determined by both water itself and materials dissolved or suspended with it, such as suspended solids, algae or phytoplankton (Civera et al., 2011; V.-Balogh et al., 2009). The lowest absorption capacity of water occurs at wavelengths between 400 and 600 nm (Delta, 2019; Fyfe, 2003; Govender et al., 2007; Watanabe et al., 2015).

Although the estimation of bathymetry using multispectral satellite imagery may not provide the accuracy attainable by based acoustic methods, it offers several advantages (Kibele & Shears, 2016). Multispectral satellite imagery is more cost- and time-effective than acoustic methods, which need expensive equipment and extensive fieldwork (Cao et al., 2024; Wicaksono et al., 2024). It makes remote sensing accessible for regions with limited resources and access (Cao et al., 2024; Ji et al., 2023; Wicaksono et al., 2024).

Satellite-derived bathymetry (SDB) utilizes remote sensing technology to analyze reflection value from the seafloor and generate bathymetric information. It has been adopted by several researchers (Guzinski et al., 2016; Hernandez & Armstrong, 2016; Jagalingam et al., 2015; Kanno et al., 2011a, 2013; Kanno & Tanaka, 2012; Manessa et al., 2016; Pacheco et al., 2015; Pushparaj & Hegde, 2017; Vinayaraj et al., 2016; Yuzugullu & Aksoy, 2014). The developed SDB algorithm assumes that the attenuation coefficient of the water is constant and that the bottom type of the water is homogeneous (Hashim et al., 2021). Therefore, the SDB accuracy is likely high in clear sea waters with homogeneous water quality and bottom type (Vinayaraj et al., 2016). However, this condition is challenging for the general Indonesian water characteristic, and accuracy remains challenging compared with the inside depth values (Setiawan et al., 2020).

Thus, this study aimed to produce bathymetry using the semiparametric regression method with spatial coordinates (Kanno-STR) and to analyze the effect of using bottom types of in-situ depth data with two modifications. The first modification is using in-situ depth data without considering the bottom cover of shallow waters. The second modification uses in-situ depth data by considering shallow waters' bottom cover, consisting of corals, seagrasses, macroalgae, and substrates. The Kanno-STR demonstrated high performance, as did Semiparametric Regression using depth-independent variables and spatial coordinates (TNP), both outperforming ten other bathymetry extraction algorithms—Ratio Transform (RT), Multiple Linear Regression (MLR), Multiple Nonlinear Regression (RF), Second-Order Polynomial of Ratio Transform (SPR), Principal Component (PC), Multiple Linear Regression with Relaxing Uniformity Assumptions on Water and Atmosphere (KNW), Semiparametric Regression using Depth-Independent Variables (SMP), Bagging Fitting Ensemble (BAG), Least Squares Boosting Fitting Ensemble (LSB), and Support Vector Regression (SVR)—when tested using SPOT 6 imagery in the Gili Mantra Islands, West Nusa Tenggara, and Menjangan Island, Bali (Manessa et al., 2018).

Hence, this study applied this method to the latest SPOT 7 satellite imagery in the shallow waters of Gili Trawangan, Gili Meno, and Gili Air, West Nusa Tenggara Province, as these areas have clear waters and contain four objects of corals, seagrasses, macroalgae, and substrates. Moreover, this study evaluated the penetrate ability of SPOT imagery in clear water. Several previous studies have extracted bathymetry by employing SPOT 7 satellite Imagery. Setiawan et al. (2020) employed Van Hengel and Spitzer method to extract bathymetry in Karimunjawa Island; it produced depth index values ranging from 0.0985 to 0.6378, demonstrating the effectiveness of SPOT 7 in the bathymetric application. Setiawan et al. (2019) employed the same satellite imagery on Gili Matra island using a random forest method with two medications with and without benthic habitat concentration; their finding shows that without benthic habitat has higher R^2 (90.2%) and RMSE (1.57) than with benthic habitat consideration. However, no study in the area employs the semiparametric regression method using spatial coordinates (Kanno-STR). In addition, this study becomes more important by considering the geographic condition and status of marine protected areas. Gili Trawangan, Gili Meno, and Gili Air are situated along the Ring of Fire, making it highly likely that the area is an

atoll, which is crucial because a home of diverse marine ecosystems, providing habitat for various aquatic species, including fish nurseries. The atoll area is unique, and a number of scientists have conducted studies on bathymetric detection in the atoll area due to its characteristic relatively shallow in the whole area (Duan et al., 2022; Poppenga, S.K., Palaseanu-Lovejoy, M., Gesch, D.B., Danielson, J.J, Tyler, 2018). Furthermore, Gili Matra is a national Marine Protected Area (MPA); hence, the outcomes of this research are expected to support conservation management in Gili Matra by delivering precise bathymetric data critical for informed decision-making.

2. Materials and Method

2.2. Location and Data

This research was carried out on Gili Trawangan, Gili Meno, and Gili Air in West Nusa Tenggara Province, which is geographically located at coordinates 8.333683 – 8.372661 South Latitude and 116.020372 – 116.094100 East Longitude (Figure 2.1). It is located in the atoll coral areas, which have clear water and consist of corals, seagrasses, macroalgae, and substrates. Moreover, it is one of the MPAs in Indonesia (Di Lazzaro et al., 2014).

SPOT 7 (Satellite Pour l'Observation de la Terre 7), launched on June 30, 2014, by Airbus Defence and Space, is a high-resolution Earth observation satellite tailored for diverse applications such as agriculture, urban planning, and environmental monitoring and was utilized to conduct this study (ESA, n.d.). It captures imagery with a 1.5-meter resolution in its panchromatic band, which provides detailed black-and-white images, and 6-meter resolution in its four multispectral bands: blue (450-520 nm) for water and atmospheric studies, green (530-590 nm) for vegetation health analysis, red (625-695 nm) for land use and vegetation mapping, and near-infrared (760-890 nm) for biomass and moisture content assessments (ESA, n.d.). With a 60-kilometer swath and sun-synchronous orbit, SPOT 7 ensures frequent, high-quality data collection and complements SPOT 6 for enhanced coverage and revisit capabilities. This study recorded the image on June 28, 2018, at 10:12:49 Central Indonesian Time. Moreover, the hydrographic data survey was collected during the field survey conducted on June 22-28, 2018, by measuring using a single beam echosounder and differential global positioning system. The most important aspect is that the time of the satellite imagery recording should coincide with the time of the field survey.

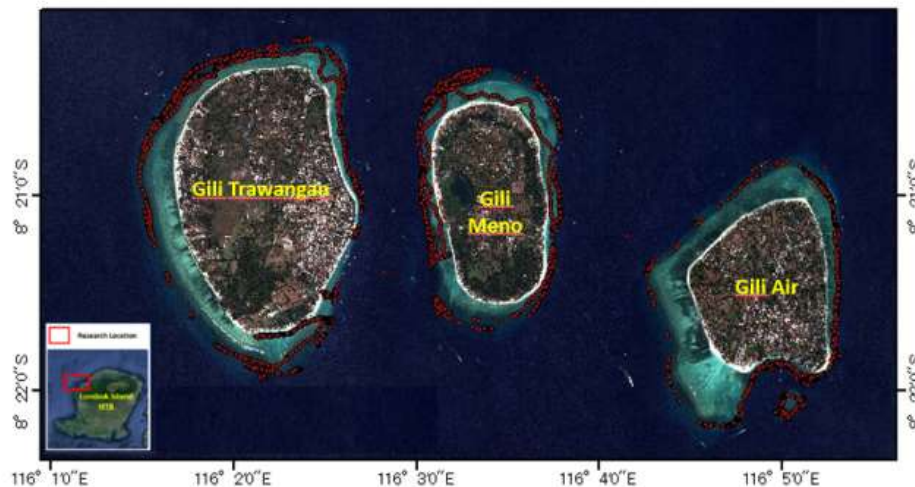


Figure 2.1. Research Location

2.3. Method

The holistic step of this study can be seen in Figure 2.2. This research was carried out through several stages of data processing, namely tidal correction, image processing, and bathymetry extraction (Ashphaq et al., 2021; Paper, 2014; Prayogo & Basith, 2021). Measured depth tidal conditions influence data from hydrographic surveys. Depth correction is based on the mean sea level. Tidal data were obtained from field surveys and tidal station records. The preliminary processing of satellite imagery includes radiometric and atmospheric correction. This stage aims to generate standardized image data for future analysis. The last stage is bathymetric extraction by the semiparametric regression method with spatial coordinates (STR). It involves deriving sea depth information from remote sensing images by analyzing the pixel values, which reflect each visible wavelength of the SPOT 7 images.

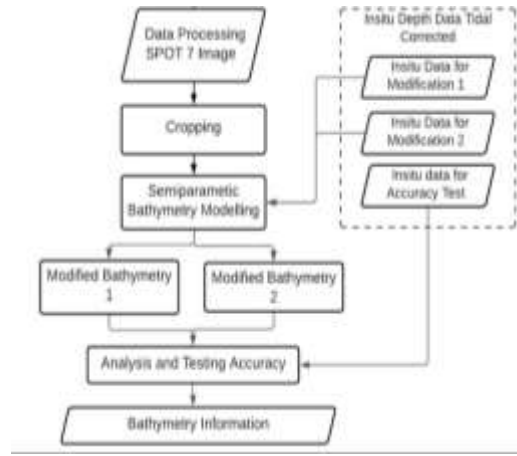


Figure 2.2. Flowchart of Study

This study analyzed the effect of reflectance on bathymetric accuracy by using in-situ depth data in the modeling process with two modifications. The first modification ignored the condition of bottom reflectance, while the second modification considered it, categorizing the bottom reflectance into corals, seagrasses, macroalgae, and substrates. This modification aimed to achieve the most accurate bathymetric detection from SPOT 7. Shallow bathymetric estimation using satellite imagery involved three main components: atmospheric conditions, bottom reflectance, and water column scatterers (Figure. 2.3).

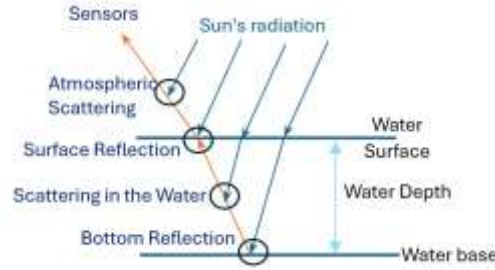


Figure 2.3. Bathymetric Extraction Concept (Kanno et al., 2011)

This concept is the basis for studying the effect of necessary cover reflectance, which is one factor that influences the estimation of bathymetry. The seafloor surface reflectance component is the main component used as a value in generating ocean depth. At the same time, the other three parts are residual or noise components that need to be removed or searched for to correct the spectral value of the image received by the satellite sensor. Reflections on all these components can be formulated as follows:

$$L(\lambda) = \{V+(B-V) \exp(-kh)\} TE+S+A \quad (1)$$

Where L is Spectral radiance, V denotes in-water scattering, B is Bottom reflectance, k represents Attenuation coefficient, h is in-situ depth, T is Atmosphere-surface transmission, E is downwelling irradiance atmosphere, S represents Surface reflection, and A is Atmosphere scattering.

Entering the value of the near-infra-red (NIR) band was considered a correction for pixel values of the blue, green, and red bands. This condition is because NIR values are entirely absorbed by water, particularly in the 700-900 nm range (Röttgers et al., 2014), causing the NIR band values to be suitable replacements for pixel values in deep-sea areas, which are considered entirely noise. The depth formula modified using the Semiparametric Regression with Spatial Coordinates (STR) method by a statistical combination of Lyzenga’s method and a spatial interpolation method is as follows (Kanno et al., 2011).

$$h = X\beta + t(z) + \epsilon' \quad (2)$$

Where: h is water depth, β represents the estimated by least squares using pixels with measured depth, $t(z)$ denotes a smooth nonparametric function of the two-dimensional coordinate vector z , and ϵ' represents the error term.

2.4.Accuracy Test

Evaluating the model's accuracy involves calculating the R^2 (R squared) and RMSE (Root Mean Square Error). This process is conducted through random cross-validation experiments, utilizing 70% of the in-situ data over 100 repetitions (Lobsey et al., 2017). The equations used to compute the determination coefficient (R^2) and RMSE are as follows:

$$R^2 = 1 - \frac{\sum_i (h_i - \hat{h}_i)^2}{\sum_i (h_i - \bar{h})^2} \quad (3)$$

$$\text{RMSE} = \left(\frac{\sum_{i=1}^n (h_i - \hat{h}_i)^2}{n} \right)^{0.5} \quad (4)$$

Where h is in-situ depth, \hat{h} represent the extraction depth form SPOT 7, \bar{h} Denotes the mean of in-situ depth and n is the amount of data.

Data accuracy analysis was conducted to determine the accuracy obtained from the absolute depth results. The accuracy of the data in this study was analysed using the confusion matrix method. The confusion matrix itself is a matrix arranged to determine the accuracy values of user accuracy (UA), producer accuracy (PA), and overall accuracy (OA) (Kulkarni et al., 2020). Mathematically, the three accuracies can be stated as follows.

$$\text{PA} = \frac{x_{ii}}{x_{i+}} \times 100\% \quad (5)$$

$$\text{UA} = \frac{x_{ii}}{x_{+i}} \times 100\% \quad (6)$$

$$\text{OA} = \frac{\sum_{i=1}^k x_{ii}}{N} \times 100\% \quad (7)$$

where: N is the number of in-situ depth data used for observations, x_{ii} the diagonal value of the i -th row and i -th column confusion matrix, x_{+i} is the number of pixels in the i -th column, x_{i+} denotes the number of pixels in the i -th row, PA_x is the producer accuracy value in a class and UA_x is the user accuracy value in a class.

In addition to calculating the overall accuracy using the confusion matrix, this study will also calculate the accuracy of the classification results using kappa analysis (Yu, 2005). Kappa analysis can be used to cover the lack of overall accuracy of the confusion matrix. The calculation of the kappa coefficient is carried out with the following equation:

$$\text{Kappa} = \frac{N \sum_{i=1}^k x_{ii} - \sum_{i=1}^k (x_{i+} x_{+i})}{N^2 - \sum_{i=1}^k (x_{i+} x_{+i})} \quad (8)$$

where: N is the total number of all pixels used for observations, k is the number of lines in confusion matrix (number of classes), x_{ii} denotes the diagonal value of the i -th row and i -th column confusion matrix, x_{+i} is the number of pixels in the i -th column and x_{i+} is the number of pixels in the i -th row. If the value of $K \geq 0.8$ indicates very good map accuracy, between 0.4 - 0.8 is in the medium category, and if the value of $K \leq 0.4$ is in the bad category (McHugh, 2012).

3. Results and Discussion

The SDB processing in this study was conducted with two modifications with and without considering the bottom surface. The modelling was performed using R32 software with a script developed by Kanno et al. (2011). The overall accuracy (OA), user accuracy (UA), producer accuracy (PA), and Kappa values were calculated based on a confusion matrix. The confusion matrix was created for five depth class intervals: 0-2 m, 2.01-5 m, 5.01-10 m, 10.01-20 m, and > 20 m. The classification based on the integrated classification from several studies that classification identified 0-2m as very shallow to shallow water depth (McCormack & Borrelli, 2023), less than 10 m was identified as intermediate shallow depths (Bagaini & Boiero, 2022; Le, 2021) and we divided into two intermediate classes i.e., intermediate 1 and 2 of shallow depths, 10-20m was grouped into deeper shallow depths (Cotter et al., 2016), and >20 m was beyond the typical shallow water (Bagaini & Boiero, 2022). Depth greater than 20 m may require a different method for detecting bathymetry. However, in this study, we observed the capacity of multispectral wavelength, which, under specific conditions, can penetrate sunlight to a depth of less than 30. Thus, we included this depth range in this classification class. Furthermore, the class intervals were established to analyze the accuracy and RMSE in greater detail for each depth class.

The first modification in this study demonstrated that the STR method could generate depth measurements up to 29.93 m, utilizing 3,375 in-situ depth data points. It achieved a high coefficient of determination (R^2) of 0.95, with the distribution result illustrated in Figure 3.1. Meanwhile, the second modification showed the STR method producing depths up to 21.03 m, also based on 3,375 in-situ depth data points. This modification generated an (R^2) of 0.84, with its distribution result in Figure 3.2. The first modification enhanced the STR method by enabling accurate depth estimation with high predictive precision.

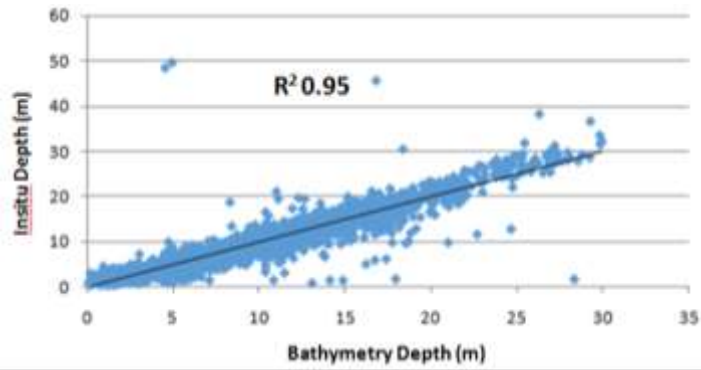


Figure 3.1. Bathymetry Results of The First Modification

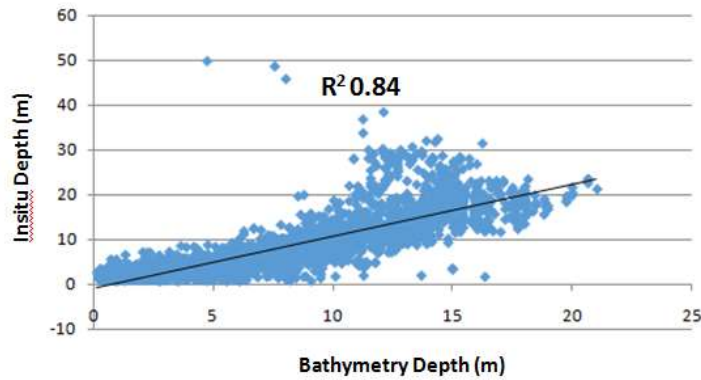


Figure 3.2. Bathymetry results of the second modification

The confusion matrix results for the five depth classes in both simulation modifications are presented in Tables 1 and 2. Absolute bathymetric was calculated using survey data, incorporating 3,375 in-situ depth points into the confusion matrix. Based on Table 1, the accuracy result for the first modification, which does not account for substrate condition, revealed an overall accuracy of 78 % for bathymetric detection from SPOT 7 imagery, with a kappa coefficient of 0.71. These results indicate that the algorithm produces bathymetry information of good quality, as an overall accuracy above 60 % is considered reliable, and a kappa coefficient between 0.4 and 0.8 falls within the medium quality range.

The RMSE value for each depth interval was calculated as follows: 1.81 m for 0-2 m, 1.06 m for 2.01-5 m, 1.79 m for 5.01 – 10 m, 2.71 m for 10 – 20 m, and 5.78 for depths greater than 20 m. the producer accuracy across these intervals was 73.35%, 75.80%, 72.89%, 91.15% and 75.82 %, respectively. Similarly, the user accuracy for each depth interval was recorded as 78.10%, 79.15%, 73.78%, 79.11% and 83.64%, respectively. These metrics highlighted the varying accuracy level of the model across different depth ranges, with the high producer accuracy observed in the 10 – 20 m interval and the high user accuracy model in the > 20 m interval.

According to Table 2, the accuracy matrix results for the second modification show an overall accuracy of 61 % for bathymetry detection using SPOT 7 imagery, with a kappa coefficient of 0.49. these results indicated that the algorithm provides bathymetry information of good quality as the overall accuracy exceeds 60 %, and the kappa coefficient falls within the range of 0.4 to 0.8, classifying it as medium quality. The RMSE values calculated for each depth interval were as follows: 2.41 m for 0–2 m, 1.89 m for 2.01–5 m, 1.99 m for 5.01–10 m, 3.49 m for 10–20 m, and 12.49 m for depths greater than 20 m. The producer accuracy for these intervals was 40.47%, 59.72%, 68.46%, 88.52%, and 2.20%, respectively. Similarly, the user accuracy was 59.26% for 0–2 m, 65.06% for 2.01–5 m, 53.97% for 5.01–10 m, 65.17% for 10–20 m, and 100% for depths greater than 20 m. These results highlighted the variability in accuracy and error across depth ranges, with high producer accuracy observed at 10 – 20 m and perfect user accuracy at depths > 20 m despite the significantly higher RMSE in this range.

Both model modifications performed better in high producer accuracy for 10 – 20 m and user accuracy > 20 m. Producer accuracy measured the probability that a reference pixel is correctly classified. In contrast, user accuracy refers to the likelihood that a pixel classified into a particular class represents that category in the field. The producer accuracy focused on the classifier’s performance, or, to say, the performance of models in this study in correcting reference pixels, while user accuracy emphasized the reliability of the classification from the user’s perspective. User accuracy indicated the pixel in the model classified as a specific category genuinely belongs to that category on the ground. The factor influenced by the > 20 class showed higher user accuracy because of their less uniqueness compared to other classes and allowing simple classification.

Table 1. Accuracy Test Results Modification 1

<i>In-situ</i> (m) \ <i>Estimation</i> (m)	0 – 2	2.01 – 5	5.01 – 10	10.01 – 20	> 20	Row Total	RMSE (m)
0 – 2	435	147	5	5	1	593	1.81 m
2.01 – 5	122	858	149	3	0	1132	1.06 m
5.01 – 10	0	77	543	124	1	745	1.79 m
10.01 – 20	0	0	39	659	25	723	2.71 m
> 20	0	2	0	42	138	182	5.78 m
Column Total	557	1084	736	833	165	3375	
Accuracy	78%						
Kappa	0,71						

Table 2. Accuracy Test Results Modification 2

<i>In-situ</i> (m) \ <i>Estimation</i> (m)	0 – 2	2.01 – 5	5.01 – 10	10.01 – 20	> 20	Row Total	RMSE (m)
0 – 2	240	280	69	4	0	593	2.41 m
2.01 – 5	161	676	281	14	0	1132	1.89 m
5.01 – 10	4	82	510	149	0	745	1.99 m
10.01 – 20	0	0	83	640	0	723	3.49 m
> 20	0	1	2	175	4	182	12.49 m
Column Total	405	1039	945	982	4	3375	
Accuracy	61%						
Kappa	0,49						

The depth results of the first modification give better results than those of the second. These results include maximum penetration depth, coefficient of determination R^2 , accuracy, and kappa coefficient. The lowest RMSE error percentage from the results of the first modification was obtained at the 10.01 – 20 m class interval, which was 13.55%. The most significant producer accuracy, which is 91.15%, is from class 10.01 – 20 m. The results of the first modified bathymetry information with the STR method made in 5-depth class intervals can be seen in Figure 3.3.

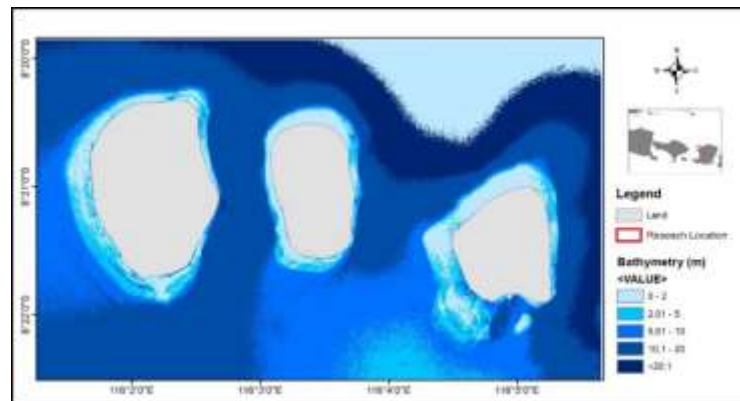


Figure 3.3. First Modified Bathymetry Information with The STR Method Made in 5 Depth Class Intervals

The finding highlighted the effectiveness of the first model modification in producing more accurate and reliable bathymetric information by using SPOT 7 in these study areas. The bathymetric results obtained from the first modification (without

considering the bottom surface) show better performance than the second modification (with considering the bottom surface) across several metrics, including maximum penetration depth, R^2 , overall accuracy, and kappa coefficient. The first modification achieved its lowest RMSE error percentage of 13.55% in the 10.01-20 m depth classification (intermediate two shallow water). The highest producer accuracy, 91.15%, was also achieved for this class. The bathymetry information generated from this first modification model by the STR method, which is classified into five depth classes, is shown in Figure 3.3. Moreover, Figure 3.3 reveals the morphology of the seabed. The bathymetric contours indicated that the northern and eastern regions are more profound than the southern areas. Shallow bathymetric contours surround all three islands. This contour distribution demonstrated the capability of SDB in identifying relatively uniform shallow bathymetric contours following the geological pattern. These islands are unique because they are formed from a single Vulcanic seabed rock composed of pillow lava featuring three elevations surrounded by coral reefs. These reefs have grown to sea level, created atolls, and formed the island.

Applying the first and second model-modified in-situ data using the Kanno-STR method caused a decline in bathymetric information accuracy. The R^2 dropped from 0.95 to 0.84, overall accuracy degenerated from 78% to 61 %, and the kappa coefficient reduced from 0.71 to 0.49. It indicated that the Kanno-ST method was designed to count for the general condition of the seabed by adding bottom cover information from the in-situ distribution, causing less significance and accuracy. Instead, the method's effectiveness depends primarily on the total amount of in-situ data available, as the machine learning iterations in the Kanno-STR script rely on sufficient data for accurate modeling. However, reducing the amount of in-situ data directly impacts the accuracy of the result (Pause et al., 2016). The accuracy may be increased by reducing the accuracy; however, in this study, we avoid it due to time-consuming with the unreliable results because the in-situ describes the detail and uniqueness of the bottom cover.

The findings of this STR model show an increase in accuracy compared to several previous studies. In Gili waters was able to map depths of up to 20 m with an R^2 value of 0.902 using SPOT-7 data and the Random Forest model (Setiawan, 2019). Ev Evagorou produced bathymetric information based on time series analysis of 12 monthly Sentinel 2 multispectral image data using the band ratio algorithm with R^2 values ranging from 0.81 to 0.95 on the Limassol coast of Cyprus (Evagorou et al., 2019). Pushparaj used the band ratio method and panchromatic Landsat 8 satellite imagery with a spatial resolution of 15 m to produce bathymetry to a depth of 10 m with an R^2 correlation of 0.8951 in the coastal waters of Mangaluru, India (Pushparaj & Hegde, 2017). Bachri using Quickbird 2 satellite imagery with a spatial resolution of 2.44 m in the shallow waters of Panggang Island was able to map depths of up to 8 m in the reef flat and lagoon areas with an R^2 value of 0.898 (Bachri et al., 2013).

When compared to the marine map No. 292.3 Tahun 2013 produced by the Navy Center for Hydro-Oceanography, the resulted image-based bathymetry map of the present study has some similarities and differences (Fig 7). Fig 7 shows several similar points on the two data set as shown in points with number 1, 2, 3, 4, 5 and 6. The Kanno-STR algorithm is able to provide depth information for shallower areas which are not detected in the marine map of the Navy Center for Hydro-Oceanography (Green Area). Fig 7 shows several different points on the two data set as shown in points with number, as shown in points number 7, 8, 9, 10 and 11. The unfavorable results of the two modifications indicate the need for improvements in carrying out special studies of bathymetry which are related to the condition of the bottom water habitat.

For Indonesia, where 77% of the territory is marine, the SDB model offers a valuable tool for exploring shallow seas and identifying bathymetric contour patterns (Dewi et al., 2019; Ramadhan et al., 2021; Sartika et al., 2018; Wulandari & Wicaksono, 2021). Furthermore, SDB can support various applications, such as locating marine tourism spots, marine parks, and diving sites, as well as other marine tourism activities (Mavraeidopoulos et al., 2018)(Westley, 2021).

For further research, we suggest adding in situ data to each area of the water base cover to determine the modeling coefficient and calculate accuracy using machine learning. In addition, developing SDB determination modeling based on analytical models. We also suggest using satellite imagery data that has a higher spatial resolution. All of this is done in order to produce SDB information with better accuracy.

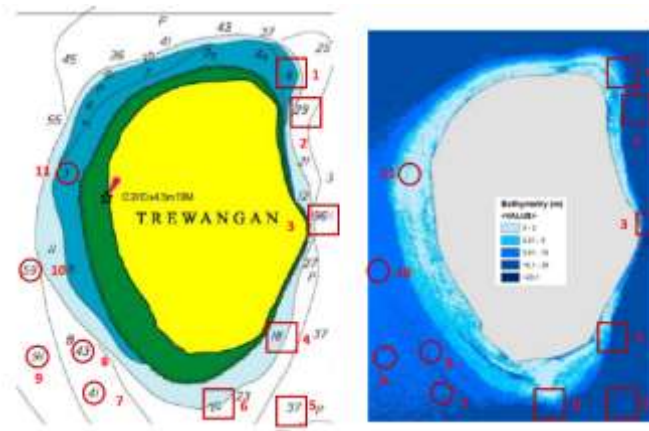


Figure 3.4. Results of Bathymetry Kanno-STR (right) with Marine Map No. 292.3 (left)

4. Conclusion

SPOT-7 satellite imagery can extract bathymetry using Semiparametric regression using spatial coordinates (STR) in the shallow waters of Gili Trawangan, Gili Meno, and Gili Air in West Nusa Tenggara Province. The results of SPOT-7 satellite image processing for bathymetry determination using the STR method produces a coefficient of determination $R^2 0.95$, an accuracy value 78 % and a kappa coefficient value is 0.71 for first modification. While the second modification produces a coefficient of determination $R^2 0.84$, an accuracy value of 61% and a kappa coefficient value of 0.49. The second modification separating the depth field data based on the cover of the benthic habitat into the coral, seagrass, macroalgae, and substrates, does not improve the accuracy of the results of the bathymetry.

5. Acknowledgment

The authors express their gratitude for the support provided by the Ministry of Research, Technology, Higher Education through the National Innovation System Research Incentive Program in 2018, Remote Sensing Applications Centre, LAPAN and Andi Besse Rimba from JICA Ogata Research Institute.

6. References

- Abdul Gafoor, F., Al-Shehhi, M. R., Cho, C.-S., & Ghedira, H. (2022). Gradient Boosting and Linear Regression for Estimating Coastal Bathymetry Based on Sentinel-2 Images. *Remote Sensing*, 14(19), 5037. <https://doi.org/10.3390/rs14195037>
- Ashphaq, M., Srivastava, P. K., & Mitra, D. (2021). Review of near-shore satellite derived bathymetry: Classification and account of five decades of coastal bathymetry research. *Journal of Ocean Engineering and Science*, 6(4), 340–359. <https://doi.org/10.1016/j.joes.2021.02.006>
- Bachri, S., Selamat, M. B., Siregar, V. P., & Wouthuyzen, S. (2013). The Comparison of Bathymetric Estimation from Three High Resolution Satellite Imagery. August, 1–11.
- Bagaini, C., & Boiero, D. (2022). Challenges and Solutions in Shallow and Deep Water Ocean Bottom Seismic. Third EAGE Marine Acquisition Workshop, 1–4. <https://doi.org/10.3997/2214-4609.202242009>
- Cao, B., Liu, H., & Cao, B. (2024). Making satellite-derived empirical bathymetry independent of high-quality in-situ depth data: An assessment of four possible model calibration data. *ISPRS Journal of Photogrammetry and Remote Sensing*, 211, 336–355. <https://doi.org/10.1016/j.isprsjprs.2024.04.014>
- Civera, J. I., Gil, I. R., Laguarda-Miro, N., Garcia-Breijo, E., Gil-Sánchez, L., & Martínez-Guijarro, R. (2011). Instrument for sunlight extinction measurement in water bodies. *Sensors and Actuators A: Physical*, 168(2), 267–274. <https://doi.org/10.1016/j.sna.2011.04.025>
- Cotter, E. D., Murphy, P., Joslin, J., Brunton, S., Stewart, A., & Polagye, B. L. (2016). Use of integrated instrumentation to detect and classify targets in shallow water. *Journal of the Acoustical Society of America*, 140(4_Supplement), 3350–3350. <https://doi.org/10.1121/1.4970704>
- Delta, G. (2019). An Examination of Spectral Reflectance Properties of some Wetland Plants in An Examination of Spectral Reflectance Properties of some Wetland Plants in Göksu Delta , Turkey. 13(December 2018), 194–203.
- Dewi, R. S., Hartanto, P., Oktaviani, N., Pujawati, I., Nursugi, N., & Aditya, S. (2019). Satellite-derived bathymetry to improve bathymetric map of Indonesia. December, 31. <https://doi.org/10.1117/12.2540779>
- Dewi, R. S., & Oktaviani, N. (2021). Shallow Water Bathymetry Extraction in Small Island of Wakatobi, Indonesia. 2021 IEEE International Geoscience and Remote Sensing Symposium IGARSS, 7374–7377. <https://doi.org/10.1109/IGARSS47720.2021.9554093>
- Di Lazzaro, M., Zarlenga, A., & Volpi, E. (2014). A new approach to account for the spatial variability of drainage density in rainfall runoff modelling. *Boletín Geológico y Minero*, 125(3), 301–314.
- Duan, Z., Chu, S., Cheng, L., Ji, C., Li, M., & Shen, W. (2022). Satellite-derived bathymetry using Landsat-8 and Sentinel-2A images: Assessment of atmospheric correction algorithms and depth derivation models in shallow waters. *Optics Express*, 30(3), 3238. <https://doi.org/10.1364/oe.444557>

- ESA. (n.d.). Earth Online. https://earth.esa.int/eogateway/search?category=news&news_type=data+release+news
- Evagorou, E., Mettas, C., Agapiou, A., Themistocleous, K., & Hadjimitsis, D. (2019). Bathymetric maps from multi-temporal analysis of Sentinel-2 data: The case study of Limassol, Cyprus. *Advances in Geosciences*, 45(1988), 397–407. <https://doi.org/10.5194/adgeo-45-397-2019>
- Fyfe, S. K. (2003). Spatial and temporal variation in spectral reflectance: Are seagrass species spectrally distinct? *Limnology and Oceanography*, 48(1 II), 464–479. https://doi.org/10.4319/lo.2003.48.1_part_2.0464
- Govender, M., Chetty, K., & Bulcock, H. (2007). A review of hyperspectral remote sensing and its application in vegetation and water resource studies. *International Water and Irrigation*, 27(3), 20–24.
- Guzinski, R., Spondylis, E., Michalis, M., Tusa, S., Brancato, G., Minno, L., & Hansen, L. B. (2016). Exploring the utility of bathymetry maps derived with multispectral satellite observations in the field of underwater archaeology. *Open Archaeology*, 2(1), 243–263. <https://doi.org/10.1515/opar-2016-0018>
- Hashim, N. S., Windupranata, W., Tahar, K. N., & Sulaiman, S. A. H. (2021). Shallow-Water Bathymetry Estimation at Pantai Tok Jembal, Terengganu, Malaysia Using Landsat 8 (OLI). *IOP Conference Series: Earth and Environmental Science*, 767(1). <https://doi.org/10.1088/1755-1315/767/1/012008>
- Hernandez, W. J., & Armstrong, R. A. (2016). Deriving bathymetry from multispectral remote sensing data. *Journal of Marine Science and Engineering*, 4(1). <https://doi.org/10.3390/jmse4010008>
- Jagalingam, P., Akshaya, B. J., & Hegde, A. V. (2015). Bathymetry mapping using landsat 8 satellite imagery. *Procedia Engineering*, 116(1), 560–566. <https://doi.org/10.1016/j.proeng.2015.08.326>
- Jawak, S. D., Vadlamani, S. S., & Luis, A. J. (2015). A Synoptic Review on Deriving Bathymetry Information Using Remote Sensing Technologies: Models, Methods and Comparisons. *Advances in Remote Sensing*, 04(02), 147–162. <https://doi.org/10.4236/ars.2015.42013>
- Ji, X., Ma, Y., Zhang, J., Xu, W., & Wang, Y. (2023). A Sub-Bottom Type Adaption-Based Empirical Approach for Coastal Bathymetry Mapping Using Multispectral Satellite Imagery. *Remote Sensing*, 15(14), 3570. <https://doi.org/10.3390/rs15143570>
- Kanno, A., Koibuchi, Y., & Isobe, M. (2011a). Shallow water bathymetry from multispectral satellite images: Extensions of Lyzenga's method for improving accuracy. *Coastal Engineering Journal*, 53(4), 431–450. <https://doi.org/10.1142/S0578563411002410>
- Kanno, A., Koibuchi, Y., & Isobe, M. (2011b). Shallow Water Bathymetry from Multispectral Satellite Images: Extensions of Lyzenga's Method for Improving Accuracy. *Coastal Engineering Journal*, 53(4), 431–450. <https://doi.org/10.1142/S0578563411002410>
- Kanno, A., & Tanaka, Y. (2012). Modified lyzenga's method for estimating generalized coefficients of satellite-based predictor of shallow water depth. *IEEE Geoscience and Remote Sensing Letters*, 9(4), 715–719. <https://doi.org/10.1109/LGRS.2011.2179517>
- Kanno, A., Tanaka, Y., Kurosawa, A., & Sekine, M. (2013). Generalized Lyzenga's Predictor of Shallow Water Depth for Multispectral Satellite Imagery. *Marine Geodesy*, 36(4), 365–376. <https://doi.org/10.1080/01490419.2013.839974>
- Kibele, J., & Shears, N. T. (2016). Nonparametric Empirical Depth Regression for Bathymetric Mapping in Coastal Waters. *IEEE Journal of Selected Topics in Applied Earth Observations and Remote Sensing*, 9(11), 5130–5138. <https://doi.org/10.1109/JSTARS.2016.2598152>
- Kulkarni, A., Chong, D., & Batarseh, F. A. (2020). Foundations of data imbalance and solutions for a data democracy. In *Data Democracy: At the Nexus of Artificial Intelligence, Software Development, and Knowledge Engineering*. Elsevier Inc. <https://doi.org/10.1016/B978-0-12-818366-3.00005-8>
- Lambach, D. (2022). Technology and the construction of oceanic space: Bathymetry and the Arctic continental shelf dispute. *Political Geography*, 98, 102730. <https://doi.org/10.1016/j.polgeo.2022.102730>
- Le, T. T. (2021). Effect of water depth on Kelvin–Helmholtz instability in a shallow water flow. *Journal of Mathematical Physics*, 62(10), 103101. <https://doi.org/10.1063/1.5145060>
- Lobsey, C. R., Viscarra Rossel, R. A., Roudier, P., & Hedley, C. B. (2017). Rs-Local Data-Mines Information From Spectral Libraries To Improve Local Calibrations. *European Journal of Soil Science*, 68(6), 840–852. <https://doi.org/10.1111/ejss.12490>
- Manessa, M. D. M., Haidar, M., Hartuti, M., & Kresnawati, D. K. (2018). Determination of the Best Methodology for Bathymetry Mapping Using Spot 6 Imagery: A Study of 12 Empirical Algorithms. *International Journal of Remote Sensing and Earth Sciences (IJReSES)*, 14(2), 127. <https://doi.org/10.30536/ijreses.2017.v14.a2827>
- Manessa, M. D. M., Kanno, A., Sekine, M., Haidar, M., & Nurdin, N. (2016). Lyzenga multispectral bathymetry formula for Indonesian shallow coral reef: Evaluation and proposed generalized coefficient. *Remote Sensing of the Ocean, Sea Ice, Coastal Waters, and Large Water Regions 2016*, 9999, 999900. <https://doi.org/10.1117/12.2240550>
- Mavraeidopoulos, B. A. K., Pallikaris, A., & Oikonomou, E. (2018). Satellite Derived Bathymetry (SDB) and Safety of Navigation. *The International Hydrographic Review*, 0(17), 7–20.
- McCormack, B., & Borrelli, M. (2023). Shallow Water Object Detection, Classification, and Localization via Phase-Measured, Bathymetry-Mode Backscatter. *Remote Sensing*, 15(6), 1685. <https://doi.org/10.3390/rs15061685>
- Mohamed, H., AbdelazimNegm, Salah, M., Nadaoka, K., & Zahran, M. (2017). Assessment of proposed approaches for bathymetry calculations using multispectral satellite images in shallow coastal/lake areas: A comparison of five models. *Arabian Journal of Geosciences*, 10(2), 1–17. <https://doi.org/10.1007/s12517-016-2803-1>
- Pacheco, A., Horta, J., Loureiro, C., & Ferreira. (2015). Retrieval of nearshore bathymetry from Landsat 8 images: A tool for coastal monitoring in shallow waters. *Remote Sensing of Environment*, 159(March 2015), 102–116. <https://doi.org/10.1016/j.rse.2014.12.004>
- Paper, W. (2014). Satellite-Derived Bathymetry. *EOMAP*, 1–11.
- Pause, M., Schweitzer, C., Rosenthal, M., Keuck, V., Bumberger, J., Dietrich, P., Heurich, M., Jung, A., & Lausch, A. (2016). In-situ / Remote Sensing Integration to Assess Forest Health—A Review. 1–21. <https://doi.org/10.3390/rs8060471>
- Poliyapram, V., Raghavan, V., Metz, M., Delucchi, L., & Masumoto, S. (2017). Implementation of Algorithm for Satellite-Derived Bathymetry using Open Source GIS and Evaluation for Tsunami Simulation. *ISPRS International Journal of Geo-Information*, 6(3), 89. <https://doi.org/10.3390/ijgi6030089>
- Poppenga, S.K., Palaseanu-Lovejoy, M., Gesch, D.B., Danielson, J.J., Tyler, D. J. (2018). Evaluating the Potential for Near-Shore Bathymetry on the Majuro Atoll, Republic of the Marshall Islands, Using Landsat 8 and WorldView-3 Imagery. *U.S. Geological Survey Scientific Investigations Report 2018-5024*, 14. <https://doi.org/10.3133/siR20185024>
- Prayogo, L. M., & Basith, A. (2021). The Effect of Sunlight Correction for Estimating Water Depth Using Rationing, Thresholding, and Mean Value Algorithms. *Rekayasa*, 14(1), 39–48. <https://doi.org/10.21107/rekayasa.v14i1.8698>
- Pushparaj, J., & Hegde, A. V. (2017). Estimation of bathymetry along the coast of Mangaluru using Landsat-8 imagery. *The International Journal of Ocean and Climate Systems*, 8(2), 71–83. <https://doi.org/10.1177/1759313116679672>
- Ramadhan, M. L., Sasmito, B., & Hadi, F. (2021). Analisis Pengaruh Nilai Kekeruhan Air Terhadap Akurasi Satellite Derived Bathymetry dengan

- Algoritma Stumpf (Studi Kasus: Pantai Kartini, Jawa Tengah). *Jurnal Geodesi Undip*, 10(2), 36–46.
- Röttgers, R., Dupouy, C., Taylor, B. B., Bracher, A., & Woźniak, S. B. (2014). Mass-specific light absorption coefficients of natural aquatic particles in the near-infrared spectral region. *Limnology and Oceanography*, 59(5), 1449–1460. <https://doi.org/10.4319/lo.2014.59.5.1449>
- Sartika, D., Hartoko, A., & Kurniawan, K. (2018). Analisis Data Batimetri Lapangan Dan Citra Landsat 8 Oli Di Perairan Selat Lepar Kabupaten Bangka Selatan (Analysis Bathymetry Field and Bathymetry Citra Landsat 8 Oli in Lepar Current Regency of South Bangka). *SAINTEK PERIKANAN : Indonesian Journal of Fisheries Science and Technology*, 13(2), 75. <https://doi.org/10.14710/ijfst.13.2.75-81>
- Setiawan, K. T., Ginting, D. N. B. R., Manessa, M. D. M., Surahman, Winarso, G., Anggraini, N., Basith, A., Asriningrum, W., Rosid, S., & Supardjo, A. H. (2020). Bathymetry extraction of empirical models using SPOT 7 satellite imagery. *IOP Conference Series: Earth and Environmental Science*, 500(1). <https://doi.org/10.1088/1755-1315/500/1/012063>
- Setiawan, K. T., Suwargana, N., Br. Ginting, D. N., Manessa, M. D. M., Anggraini, N., Adawiah, S. W., Julzarika, A., Surahman, S., Rosid, S., & Supardjo, A. H. (2019). Bathymetric Extraction from SPOT 7 Satellite Omagery Using Random Forest Methods. *International Journal of Remote Sensing and Earth Sciences (IJReSES)*, 16(1), 23. <https://doi.org/10.30536/j.ijreses.2019.v16.a3085>
- V.-Balogh, K., Németh, B., & Vörös, L. (2009). Specific attenuation coefficients of optically active substances and their contribution to the underwater ultraviolet and visible light climate in shallow lakes and ponds. *Hydrobiologia*, 632(1), 91–105. <https://doi.org/10.1007/s10750-009-9830-9>
- Vinayaraj, P., Raghavan, V., & Masumoto, S. (2016). Satellite-Derived Bathymetry using Adaptive Geographically Weighted Regression Model. *Marine Geodesy*, 39(6), 458–478. <https://doi.org/10.1080/01490419.2016.1245227>
- Watanabe, S., Laurion, I., Markager, S., & Vincent, W. F. (2015). Abiotic control of underwater light in a drinking water reservoir: Photon budget analysis and implications for water quality monitoring. *Water Resources Research*, 51(8), 6290–6310. <https://doi.org/10.1002/2014WR015617>
- Westley, K. (2021). Satellite-derived bathymetry for maritime archaeology: Testing its effectiveness at two ancient harbours in the Eastern Mediterranean. *Journal of Archaeological Science: Reports*, 38(May), 103030. <https://doi.org/10.1016/j.jasrep.2021.103030>
- Wicaksono, P., Djody Harahap, S., & Hendriana, R. (2024). Satellite-derived bathymetry from WorldView-2 based on linear and machine learning regression in the optically complex shallow water of the coral reef ecosystem of Kemujan island. *Remote Sensing Applications: Society and Environment*, 33, 101085. <https://doi.org/10.1016/j.rsase.2023.101085>
- Wulandari, S. A., & Wicaksono, P. (2021). Bathymetry mapping using PlanetScope imagery on Kemujan Island, Karimunjawa, Indonesia. *IOP Conference Series: Earth and Environmental Science*, 686(1). <https://doi.org/10.1088/1755-1315/686/1/012032>
- Yu, C. H. (2005). Test-retest reliability. In Kempf-Leonard, K. (ed.). *Encyclopedia of Social Measurement*, 3, 777–784.
- Yuzugullu, O., & Aksoy, A. (2014). Generation of the bathymetry of a eutrophic shallow lake using WorldView-2 imagery. *Journal of Hydroinformatics*, 16(1), 50–59. <https://doi.org/10.2166/hydro.2013.133>